Photolysis and Deacylation of Inhibited Chymotrypsin[†,‡]

Barry L. Stoddard,[§] John Bruhnke,[∥] Paula Koenigs,[∥] Ned Porter,[∥] Dagmar Ringe,[*,§] and Gregory A. Petsko[§]

Department of Chemistry, Massachusetts Institute of Technology, Cambridge, Massachusetts 02139, and Department of Chemistry, Duke University, Durham, North Carolina 27706

Received October 2, 1989; Revised Manuscript Received April 11, 1990

ABSTRACT: Inhibited chymotrypsin was reactivated through the photolysis of the covalently bound light-reversible cinnamates described in our previous paper [Stoddard, B. L., Bruhnke, J., Porter, N. A., Ringe, D., & Petsko, G. (1990) *Biochemistry 29*, 4871–4879]. The light-induced deacylation was accomplished both in solution and in protein crystals, with the release of inhibitor from the crystal monitored and confirmed by X-ray diffraction. The product of photolysis has been characterized as a 3-methylcoumarin, leading to a mechanism for light-driven deacylation of an internal lactonization that is dependent on the presence of an internal hydroxyl nucleophile. The acyl enzyme formed from cinnamate A is not suitable for photochemical studies, as the complex has a short half-life in solution and does not have a chromophore that is well separated from protein absorbance. Cinnamate B, with a *p*-diethylamino substituent, shows an enzyme deacylation rate enhancement of 10^9 for the cis photoisomer relative to the trans starting material. The half-life and deacylation rate of this compound in the E–I complex after photon absorption have been directly measured by subsecond UV absorption studies. X-ray diffraction studies of photoactivation using a flow cell show that the cinnamate B acyl enzyme complex is fully capable of light-induced isomerization and regeneration of native enzyme in the crystalline state. The E–I complex formed upon binding of cinnamate A, however, shows little if any effect from irradiation due to competitive absorbance by the highly concentrated protein at the shorter UV wavelengths. Photolysis of cinnamate B appears to occur on a time scale fast enough for applications in crystallographic studies of enzymatic intermediate-state structures.

We have previously reported the 1.9-Å structures of chymotrypsin inhibited with two *trans*-α-methylcinnamate nitrophenyl esters and discussed the observed differences in the kinetics of acylation and nonphotochemical deacylation for the two compounds. The inhibitors bind in the specificity pocket of the enzyme with a nonproductive planar conformation that prevents the oxyanion hole from properly stabilizing the transition state during catalysis. For both structures, resonance serves to deactivate the carbonyl group toward nucleophilic attack. Thus, both compounds form a covalent adduct to the active-site serine and show unusual thermal stability after binding toward deacylation and hydrolysis relative to similar phenyl substrates.

In addition to acting as competitive inhibiors of chymotrypsin and of serine proteases in general, *trans*-cinnamates possess the property of being photoisomerizable and therefore light-dissociable from the enzyme–inhibitor complex. The purpose of the work described here is to investigate the photochemical properties of these compounds and the effect of binding to the enzyme on these properties and the kinetics of isomerization, deacylation, and regeneration of enzymatic activity and to examine the possibility of using such compounds to rapidly generate free enzyme in the protein crystal without damaging or destroying the crystal itself.

Photoreversible inhibitors have been reported in the literature for years, although in some cases the photosensitivity of such compounds was discovered rather fortuitously. For example, proflavin can be photochemically reduced to a diaminoacridan product with a substantially reduced binding constant to chymotrypsin (Berezin et al., 1974); similar studies have been reported using the cis/trans isomerization of the protease inhibitor *N*-phenyl-*N*-[*p*-(phenylazo)phenyl]carbamyl chloride to produce a light-induced enzyme reactivation (Kaufman et al., 1968). It has also been shown that various substituted azophenyl compounds such as *O*-[*N*-[*p*-(phenylazo)phenyl]carbamyl]choline act as regulators of acetylcholinesterase activity and also undergo a light-dependent isomerization that directly affects their biological activity (Battels et al., 1971; Bieth et al., 1970).

Cinnamic acid derivatives were first investigated as photoreversible inhibitors of chymotrypsin by Berezin et al. (1970). The *p*-nitrophenyl ester of *cis*-4-nitrocinnamic acid (NPNC) was seen to acylate chymotrypsin to yield an E–I complex with a deacylation rate of 1.7×10^{-5} s^{-1}. Isomerization by UV light increases this rate by over 4000 times. *trans*-Cinnamic acid compounds have been studied by several groups for their ability to serve as photoreversible covalent inhibitors of serine proteases, including thrombin (Turner et al., 1987), chymotrypsin (Varfolomeyev et al., 1971), trypsin, and factor Xa (Turner et al., 1988). It has been shown (Porter & Bruhnke, 1989a) that a *p*-amidinophenyl ester of an *o*-hydroxycinnamate with a *p*-diethylamino-substituted chromophore inhibits thrombin and shows a nonphotochemical deacylation of 10^{-6} s^{-1}, whereas photolysis of this trans isomer generates an enzyme-bound cis intermediate that deacylates with a rate of 2.4×10^3 s^{-1}, giving a rate ratio for deacylation of greater than 10^9 for the geometric isomers. This rate acceleration is dependent on the

[†] Solution studies were supported by a grant from PHS (HL-17921). Flash photolysis experiments and analyses of the data produced were performed at the Center for Fast Kinetics Research, which is supported jointly by the Biomedical Research Technology Program of the Division of Research Resources of NIH (RR00886) and by the University of Texas at Austin. Crystallographic studies were supported in part by a grant from Payload Systems, Inc., of Cambridge, MA. One of the researchers (B.L.S.) is supported by a fellowship from the Whitaker College Health Fund Fellowship at MIT.

[‡] The coordinates of the photolysis product of cinnamate B have been submitted to the Brookhaven Protein Data Bank (entry 5GCH).

* To whom correspondence should be addressed.

[§] Massachusetts Institute of Technology.

[∥] Duke University.

0006-2960/90/0429-8042$02.50/0

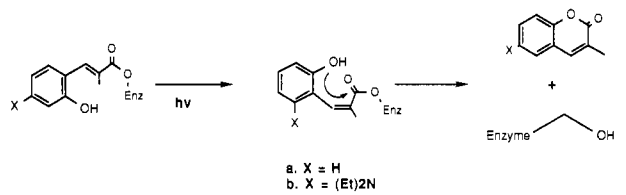

FIGURE 1: Mechanism of photolysis of *o*-hydroxycinnamates (Porter & Bruhnke, 1989a,b).

presence of the *o*-hydroxyl group, and the deacylation has been shown to proceed by an intramolecular lactonization to produce an inactive coumarin byproduct, according to the mechanism for photolysis and light-induced deacylation shown in Figure 1. Porter and Bruhnke (1989b) have gone on to show that thrombin modified with the acyl cinnamate can be used to produce light-induced blood plasma coagulation in vitro. This photodependent regeneration of enzymatic activity under physiological conditions proceeds with virtually 100% recovery of active enzyme and shows linear initial slope kinetics for coagulation time vs thrombin concentration.

On the basis of these results, a nitrophenyl ester of *trans*-hydroxymethylcinnamate specific for chymotrypsin was synthesized for the purpose of acting as a light-driven trigger in the protein crystal. This paper reports the results of our kinetic and structural studies of the light-induced reactions of chymotrypsin–cinnamate complexes. We have examined the absorption and the isomerization kinetics for the inhibitors and the photodeacylation of both bound inhibitors, both in solution and in the crystalline state, and we have tried to relate our results to the measured spectral characteristics of the systems as well as to the structural results reported previously. We are interested in the efficiency of isomerization and deacylation of the inhibitors, in how the light-dependent properties of this system can be altered by the addition of a specific chromophore (an *N*,*N*-diethylamino group), and in whether efficient photolysis can be accomplished in the crystalline system without adversely affecting the integrity of the crystal.

Materials and Methods

The synthesis and analysis of the cinnamates, growth of chymotrypsin crystals, and inhibition of crystalline chymotrypsin have been reported previously (Stoddard et al., 1990).

Solution Studies of Photoactivation

The reaction of cinnamates A and B with chymotrypsin was monitored by chromogenic assay using S-2586 (MeO-Suc-Arg-Pro-Tyr-*p*-nitroanilide hydrochloride) as described previously (Stoddard et al., 1990). A 25-fold excess of cinnamate with chymotrypsin at 1.5 μM in 30 mM Tris buffer, pH 7.4, leads to complete loss of chymotrypsin activity in less than 6 h. For cinnamate B, gel filtration of the resulting inactive chymotrypsin solution on Sephadex G-25 with pH 7.4 Tris buffer solvent gave an inhibitor-free fraction eluting identically with active chymotrypsin but with less than 2% activity. In the dark, chymotrypsin activity of this solution increased in a clean first-order process as described in the previous paper with rate constants of deacylation for the inhibitors of approximately 10^{-6} s^{-1}. Cinnamate A, however, deacylates in the dark with a rate constant 1000-fold higher than for the amino-substituted compound, making it impossible to obtain an inhibitor-free acyl enzyme from the gel filtration column that has not regained significant enzyme activity. This made accurate solution photochemical studies of the acyl enzyme from cinnamate A virtually impossible, leading us to perform detailed kinetic solution studies of photoactivation on the cinnamate B acyl enzyme (see below). UV absorption spectra

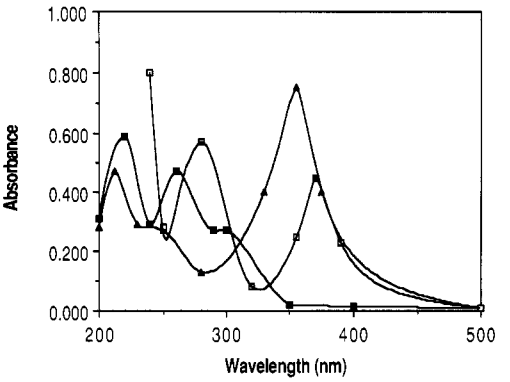

FIGURE 2: UV absorption of ethyl cinnamates A (■) and B (▲), 4 × 10^{-5} M, and cinnamate B acyl enzyme complex (□), 2 × 10^{-5} M, in Tris buffer, pH 7.4.

for both cinnamates (as their ethyl esters at 40 μM) were measured at pH 7.4 in 50 mM Tris and 150 mM NaCl buffer. These spectra are shown in Figure 2.

Nonkinetic chemical studies of the light-induced regeneration of free enzyme from the E–I complex were carried out by using two methods: (1) chromogenic assay of the irradiated enzyme to measure the recovery of activity after photolysis and (2) quantitation and analysis of the released product using gas chromatography, fluorescence, and NMR spectroscopy. Enzymatic activity was measured by the chromogenic assay using S-2586 as described previously on aliquots removed from the photolysis cell at specific time points during irradiation, as shown in Figure 4. Photolysis was performed with the focused beam of a 500-W mercury–xenon arc lamp (exit slit = 1 mm) trained on a stirred solution of acyl enzyme at 1.7 μM concentration in 50 mM Tris-HCl and 150 mM NaCl buffer at pH 7.4 and 20 °C.

Subsecond kinetic UV absorbance studies of the photolysis of the cinnamate B–chymotrypsin complex were performed in order to measure the rate of isomerization and deacylation of the inhibitor and the formation of coumarin as a function of time. The reaction was initiated with a 10-ns pulse from a Nd/YAG laser on a 23 μM acyl enzyme sample at pH 7.4, and the spectrum of the solution was monitored at 400 nm after the initiating pulse. This experiment allowed the instantaneous photolysis of the entire sample and provided a kinetic profile of the photochemical process over a 4-ms time course.

Fast photochemical studies of cinnamate A were made impossible by the fact that the acyl enzyme derived from this substrate had an absorbance in the UV which overlapped with the protein absorbance and by the instability of the acyl enzyme. The absorbance of cinnamate B was red-shifted relative to that of cinnamate A, and the acyl enzyme derived from cinnamate B (acyl enzyme B) had a λ_{max} at 380 nm, well removed from the protein absorbance. The UV spectrum of purified acyl enzyme B is also shown in Figure 2. The ϵ at 380 nm for the acyl enzyme is 18 900.

Crystallographic Studies of Photoactivation

Crystals of chymotrypsin inhibited with either cinnamate A or B were mounted in flow cells constructed from 1.5-mm-diameter quartz capillaries. This apparatus is constructed so that mother liquor may be flowed through the crystal at a controlled rate by use of hydrostatic pressure while at the same time collecting X-ray data and, in our case, irradiating the crystal with a high-intensity light source. The advantages of mounting the crystal in a flow cell are 3-fold: substrate, inhibitor, or cofactor may be introduced to the crystal in a controlled manner during data collection; reaction products

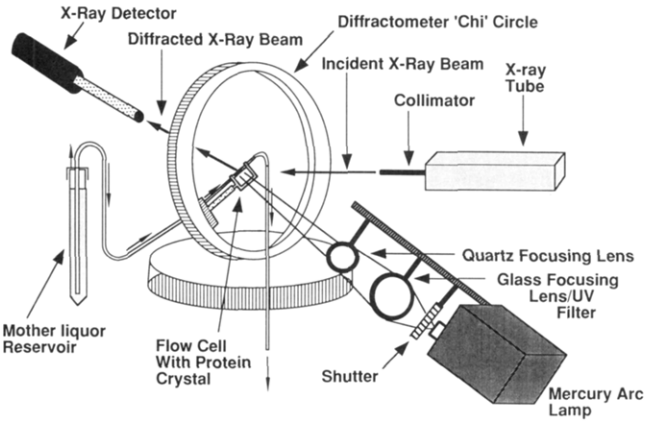

FIGURE 3: Diffractometer set-up for crystallographic flash/flow experiment.

are washed out of the crystal, thus driving the enzyme-catalyzed equilibrium in one direction; and finally, a protein crystal often proves to be more stable to radiation damage when it is continually washed with fresh mother liquor. This is important in our system, where the crystal is not only exposed to X-rays but also irradiated with high-intensity UV/visible light. (See Figure 3 for a schematic of the total experimental setup.)

The flow cell was mounted on the diffractometer and the crystal was optically aligned and centered. The flow of mother liquor was adjusted to approximately 6 mL/h, and base-line data for six chosen reflections[1] were collected in the dark continuously for 2 h. Reflections were chosen that appeared to be sensitive to changes in the active site of the enzyme. This was done by comparing the measured X-ray data for the inhibited complexes with intensities calculated from the refined protein models with the cinnamates deleted. The criteria used to choose reflections for monitoring during photolysis were resolution, strength of the measured intensities, and the percent predicted change in intensity when the inhibitor is removed from the structure. Only reflections between 4.0- and 2.2-Å resolution, with an observed intensity greater than the mean value for the data set and with a calculated change of greater than 5 times the standard deviation for that particular reflection, were considered for monitoring.

The crystal was then irradiated with the beam of a 200-W mercury–xenon arc lamp (Bausch and Lomb) for 30 min (cinnamate A) or 10 min (cinnamate B) while continuously monitoring a single reflection. The beam from the lamp was tightly focused through a pair of optical-grade lenses (Melles Griot, Irvine, CA). The first lens was a double-convex glass lens (grade BK7, 75-mm diameter, 10-mm thickness, 100-mm focal length), while the second was a single-convex quartz lens (grade UV, 25-mm diameter, 10-mm thickness, 75-mm focal length). The glass lens served both to focus the beam and also as a filter against damaging ultraviolet wavelengths (150–300 nm).

For cinnamate A, where the λ_{max} occurs at approximately 308 nm, the glass lens was replaced with a quartz lens and a water filter. In both cases, the beam incident on the crystal was focused to a diameter of approximately 3 mm, so that the crystal received approximately 50% of the total flux from the lamp. In no case was any measurable physical or crystallographic damage of the specimen observed that might have been caused by the lamp. The rate of radiation decay during collection of the full data set after irradiation appeared to be unaffected, as was the average intensity of the base-line data that were remeasured after photolysis. The crystals showed no change in appearance after irradiation.

In order to monitor a single reflection during irradiation (in hopes of detecting deacylation and loss of inhibitor), a 1° ω scan and individual background measurements were performed for each measurement of the reflection intensity. The scans were made at 3°/min with 10 s spent on background for a total of 30 s for each reflection. The entire experiment was carried out twice for both inhibitors (using new crystals each time) in order to reproduce timing curves and to monitor different reflections. After the completion of irradiation for each crystal, the full set of six base-line check reflections was remeasured continuously for 2 h to provide a postphotolysis base line for statistical comparison. Finally, after irradiation a 2.7-Å data set of the enzyme was collected for both inhibitors, and protein maps were calculated and examined to confirm the loss or retention of the inhibitor. All data were collected with the crystals mounted in the flow cells, using an appropriate octant of reciprocal space to avoid swinging the brass yoke into the path of the X-ray beam. Since only 45° of data on ϕ is necessary for a complete data set, this posed no problem. Only one crystal was necessary to collect all the data out to 2.7-Å resolution, as radiation decay during data collection was minimized by the continuous flow of mother liquor through the crystal. This flow rate was adjusted to about 1 mL/h during postphotolysis data collection. Data were collected at 20 °C on a Nicolet four-circle diffractometer with a sealed-tube X-ray generator running at 45 kV, 35 mA. All data were collected by using an ω scan as described above but with the scan rate adjusted to 2°/min for a total of 40 s/reflection. Corrections for absorption by the specimen were made by collecting absorbance curves over 360° on ϕ and ignoring measurements where the flow cell interfered with the X-ray beam. The resulting curve was used to correct the entire data set. As with the previous non flow cell data sets, these effects were minimal. Five standard reflections were remeasured for each 300 measurements to monitor and correct for radiation decay; the individual decay curves were in all cases extremely linear (95% correlation or higher), and no crystal experienced more than 10% decay over the total extent of data collection. Friedel pairs were not collected due to the high quality of the data.

Initial maps were calculated as $2F_o - F_c$ Fourier difference syntheses, by using initial chymotrypsin coordinates taken from the Brookhaven Protein Data Bank (entry 2GCH) for the structure of uncomplexed γ-chymotrypsin (Cohen et al., 1981). No inhibitor coordinates were included in the Fourier synthesis. These same conditions produced maps for our earlier structural studies, which clearly showed inhibitor binding to the active-site serine (Stoddard et al., 1990). The photolysis products were refined by using the restrained least-squares method (PROLSQ) (Konnert & Hendrickson, 1980). The refinements were completely independent of one another except for the use of the same starting coordinates.

RESULTS

Solution Studies of Photoactivation

UV Absorbance of the Inhibitors. Cinnamate A (no amino chromophore) gives a UV absorption spectrum with a shoulder at approximately 302 nm with a molar absorptivity of 6200. In contrast, cinnamate B (*p*-diethylamino) has a strong peak shifted to approximately 360 nm that shows an increase in ϵ

[1] For cinnamate A, these were (0,10,22), (13,13,25), (0,5,29), (6,17,8), (3,20,0), and (2,9,17). For cinnamate B, these were (13,20,11), (12,12,7), (14,18,1), (10,15,15), (11,11,33), and (1,22,0).

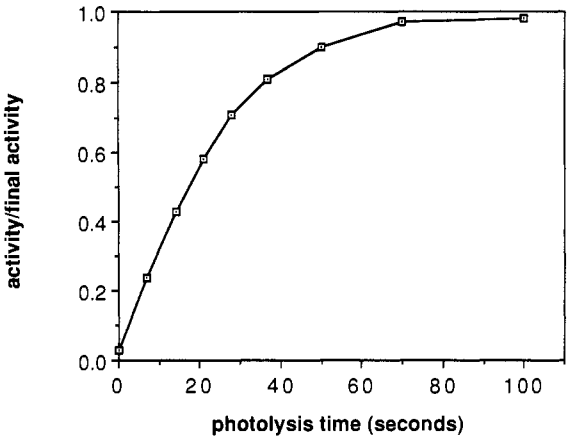

FIGURE 4: Regeneration of enzyme activity after photolysis of cinnamate B acyl enzyme. A 1.7 μM acyl chymotrypsin solution was irradiated for known amounts of time with 366-nm light through a 1-cm path length. The photoactivation was followed by chromogenic assay of chymotrypsin activity, which was performed several minutes after removal of a timed aliquot. The light source was a 500-W mercury–xenon lamp with monochromator entrance and exit slit widths set at 1 mm. The photolysis was performed at 20 °C with stirring in a buffer medium of 50 mM Tris-HCl and 150 mM NaCl, pH 7.4.

of almost 4-fold, to 22 400 mol^{-1} L cm^{-1} (Figure 2). The spectrum of this inhibitor bound to chymotrypsin shows an additional red shift to 380 nm, with a molar absorptivity of 18 900. Thus inhibitor B has the advantage that it absorbs in the UV in a readily accessible region (Hg line at 366 nm, Nd/YAG line at 355 nm) where there is no competing protein absorption.

Chromogenic Assays of Activity Regeneration and Characterization of Photolysis Product. Photolysis of acyl enzyme B (2.0 μM in Tris buffer, pH 7.4) with monochromatic 366-nm light from a 500-W high-pressure mercury arc for 75 s leads to the formation of fully active enzyme and exactly 1 equiv of 7-(*N*,*N*-diethylamino)-3-methylcoumarin (DMC) as determined by gas chromatography, fluorescence of the coumarin at 480 nm, proton and ^{13}C NMR, and elemental analysis. Thus the product ratio of *trans*-cinnamic acid (the product of the nonphotochemical deacylation) to coumarin after photolysis is approximately 0, showing that competing nonphotochemical turnover of the inhibitor is not a problem with this compound. Figure 4 shows the regeneration of enzymatic activity for inhibitor B after irradiation with 366-nm light.

The product was characterized as follows: 300-MHz ^1H NMR ($CDCl_3$) δ 7.33 (s, 1 H, coumarin 4-position), 7.15 (d, 1 H, coumarin 5-position, J = 8.8 Hz), 6.51 (dd, 1 H, coumarin 6-position, J = 2.4, 8.8 Hz), 6.45 (d, 1 H, coumarin 8-position, J = 2.4 Hz), 3.38 (q, 4 H, NCH_2, J = 7.1 Hz), 2.08 (s, 1 H, $C{=}CCH_3$), 1.18 (t, 6 H, NCH_2CH_3, J = 7.1 Hz); ^{13}C NMR ($CDCl_3$) δ 163.39, 155.71, 149.68, 139.96, 127.76, 118.13, 108.56, 97.30, 44.69, 16.76, 12.42; UV (H_2O) λ_{max} = 380 nm; mp 72 °C. Anal. Calcd for $C_{14}H_{17}NO_2$: C, 72.70; H, 7.41; N, 6.60. Found: C, 72.59; H, 7.43; N, 6.14.

Fast Kinetic Studies of Photolysis and Deacylation. Flash photolysis (10 ns) of the acyl enzyme B in Tris buffer with 355-nm light from a Nd/YAG laser results in an immediate decrease in absorbance in the range 360–400 nm, followed by a first-order increase in absorbance as the coumarin forms. The time course of flash photolysis of acyl cinnamate B as monitored by A_{400} is shown in Figure 5. We interpret this absorbance time course as resulting from photoisomerization of the trans acyl enzyme B followed by a nonphotochemical lactonization of the cis acyl enzyme B to coumarin product (see Discussion). The half life of the cis isomer after the flash

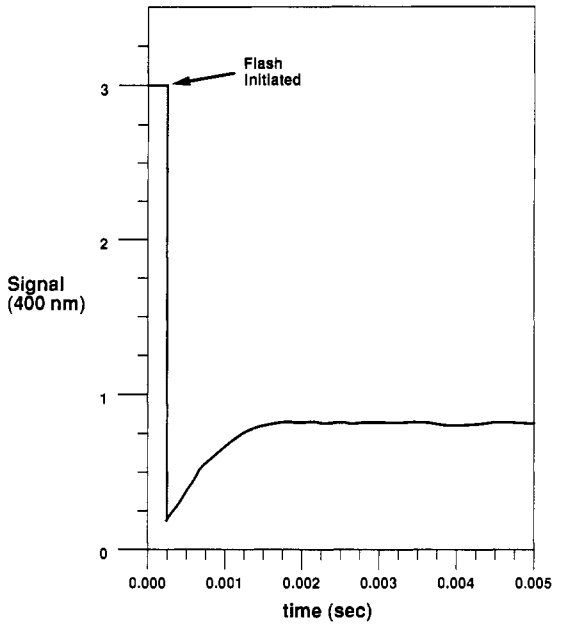

FIGURE 5: Flash photolysis of acyl enzyme cinnamate B. A 10-ns pulse at 355 nm from a Nd/YAG laser was used. The signal is the absorbance measured at 400 nm. The acyl enzyme concentration was 23 μM in Tris buffer, pH 7.4.

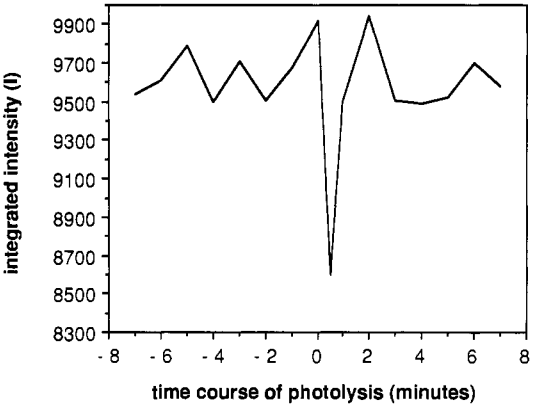

FIGURE 6: Crystallographic flow cell data for chymotrypsin–cinnamate A flash experiment. Crystalline chymotrypsin inhibited with cinnamate A was irradiated with the focused beam of a 500-W mercury arc for 30 min while being washed with mother liquor. Note the transient loss of diffraction intensity from the crystal and the return to the preflash value. The inhibitor is found to still be bound in the active site after photolysis (Figures 8 and 9).

is approximately 0.2 ms, which gives a first-order rate constant for lactonization of the cis acyl enzyme B to coumarin of approximately 3.5 × 10^3 s^{-1}.

Crystallographic Studies of Photoactivation

Photolysis of Cinnamate A. Immediately upon irradiation with the beam of a mercury arc lamp, crystals of γ-chymotrypsin inhibited with the unsubstituted cinnamate show a sharp dip in the integrated intensity of the reflection being monitored, which then returns to the base-line value (Figure 6). Photolysis was initiated by opening a shutter rather than directly firing the cold arc lamp in order to expose the crystal to a steady, reproducible flux of photons. This loss of diffraction from the crystal is observed instantaneously when the shutter is opened. The effect is common to all species of chymotrypsin crystals (unsoaked with peptide in the active site, cinnamate-inhibited, and native after cinnamate deacylation) and does not appear to be caused by isomerization of the inhibitor (see below). Repeated closing and opening of the

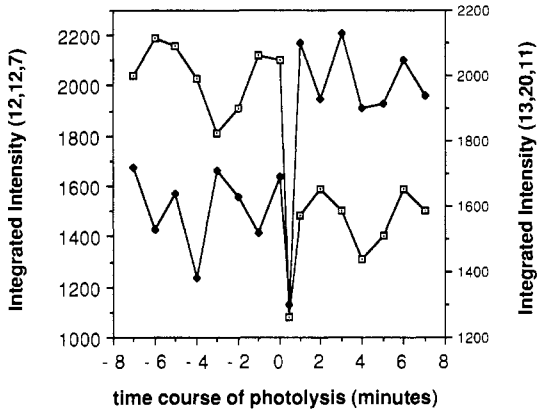

FIGURE 7: Crystallographic flow cell data for chymotrypsin–cinnamate B flash experiment. The experiment was carried out as described for cinnamate A. The total irradiation time was 10 min. The same transient loss of diffraction intensity is seen for the reflection measured during the flash initiation, and both reflections return to new base-line values within one measurement.

shutter is capable of reproducing this effect, which appears to be caused by a transient disordering of the crystal lattice upon initiation of irradiation. This is supported by the effect of true subsecond flash photolysis on the peak profiles observed for polychromatic diffraction patterns from chymotrypsin crystals, where a transitory streaking of the reflections is observed when the flash is performed simultaneously with data collection (Stoddard et al., unpublished results). Further irradiation does not significantly affect the strength of the reflection, even when the lamp is left on for up to 30 min. The intensity also does not change measurably upon termination of irradiation. The unit cell dimensions are unchanged to within ±0.1 Å after photolysis. It is not known whether the disordering effect is general for all (or most) crystalline proteins; however, similar experiments performed on the *ras* p21 protein have shown disordering of the crystals after irradiation (Almo et al., unpublished results).

After photolysis, a 2.7-Å data set was collected on the crystal in the flow cell as described in the previous section. The resulting electron density map (Figures 8 and 9) shows that the inhibitor is still covalently bound in the active site of the enzyme. The conformation of the compound appears to be completely unchanged by irradiation, with the double bond clearly trans, the phenyl ring anchored in the specificity pocket, and the carboxyl oxygen pointing away from the oxyanion hole. The surrounding protein structure appears to be unaffected, with the catalytic triad in the same orientation as for the original inhibitor-bound structure, and the location of the peptide surrounding the binding pocket is unchanged. The bond length of the serine γ-oxygen to the cinnamate carboxyl group appears to be unchanged at approximately 1.5 Å, with a planar trigonal geometry observed for the cinnamate carbon atoms and an interbond angle at the serine γ-oxygen of 115° and at the cinnamate carbonyl of 120°.

The structure from this unsuccessful attempt at photolysis was refined, starting with the initial γ-chymotrypsin coordinates from the PDB (Protein Data Bank) as described earlier, with the inhibitor included explicitly in the structure. The final *R*-factor was 17.3% at 2.7-Å resolution with no water molecules included in the structure. The final refined structure with bound inhibitor present differed from the original chymotrypsin–cinnamate A structure by an rms difference of 0.18 Å between α-carbons, as opposed to an average difference with the PDB starting coordinates of 0.26 Å. At the suggestion of a reviewer, this refinement was repeated with the inhibitor completely unrestrained; the final coordinates of this second independent refinement show virtually no change in the position of the inhibitor (rms difference less than 0.05 Å for the bound cinnamate coordinates).

Photolysis of Cinnamate B. Crystals of chymotrypsin inhibited with the substituted cinnamate also show a transient loss of diffraction intensity when irradiated with the arc lamp beam; however, the intensity of the monitored reflection then returns to a significantly different base-line value (Figure 7). The directions of the changes for the reflections shown in the figure [the (12,12,7) and the (13,20,11) reflections] agree with the changes predicted from comparison of the observed inhibitor data with calculated "native" data. The time necessary for the diffraction change to reach completion is faster than the rate at which a measurement can be repeated (less than 30 s).

As with cinnamate A, a 2.7-Å data set was collected on the crystal in the flow cell after irradiation was complete. In this case, however, the resulting electron density map (calculated in a manner identical with all previous initial maps, as a $2F_o - F_c$ difference Fourier synthesis using uncomplexed γ-chymotrypsin from the PDB for starting coordinates) shows that the cinnamate inhibitor has disappeared, leaving behind clear protein density that terminates at the γ-oxygen of serine 195 (Figure 10). The density within the specificity pocket remains clean even when the map is examined at a contour value close to the noise level of the map. The small fragment of electron density remaining in the specificity pocket could be either the remains of a very small percentage of nonphotolyzed inhibitor

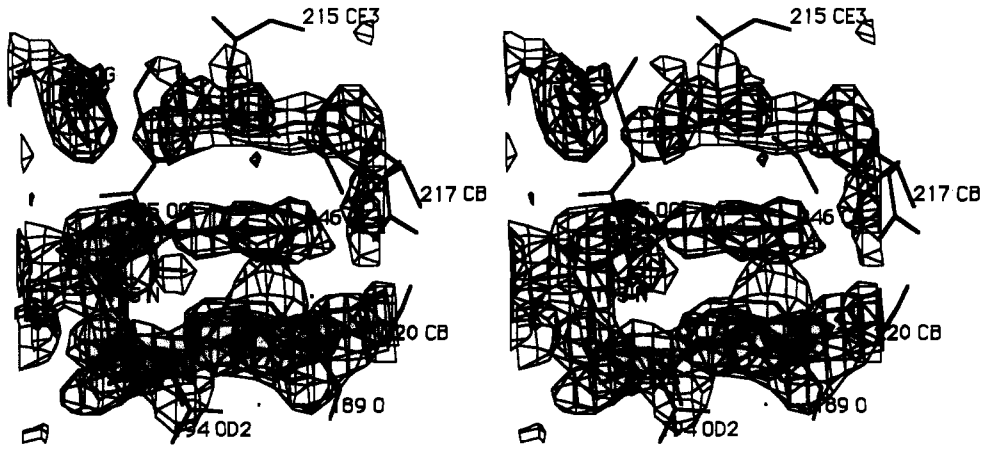

FIGURE 8: Structure of active site of chymotrypsin bound to cinnamate A after irradiation, viewed into the edge of the inhibitor. The structure of acyl enzyme is completely isomorphous with the original prephotolysis structure.

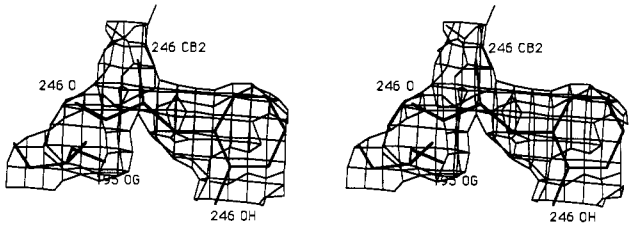

FIGURE 9: Structure of chymotrypsin inhibited with cinnamate A after irradiation, viewed perpendicular to the plane of the inhibitor ring. Note the trans geometry of the inhibitor, the covalent bond to serine 195, and the orientation of the carboxyl oxygen away from the oxyanion hole.

Table I: Summary of Data Sets and Refined Photolysis Product Structures

	cinnamate A	cinnamate B
resolution	50–2.7 Å	50–2.7 Å
no. reflcns	4015	4173
low-intensity cutoff	2σ	2σ
crystals/data set	1	1
total radiation decay	9%	10%
symmetry mates collected	245	262
symmetry R-factor	5.9%	4.7%
mean F/σ ratio	7.5	9.0
total non-hydrogen atoms	1824	1814
total water molecules	0	0
initial overall R^a	40.7%	38.3%
final overall R	17.3%	15.6%
total distances	6048	6200
total nonideal distances[b]	638	521
bond distance rms/σ	0.018/0.020	0.017/0.020
planar group rms/σ	0.024/0.020	0.022/0.020
chiral center rms/σ	0.213/0.020	0.187/0.150
nonbonded contact rms/σ		
single torsion	0.242/0.500	0.242/0.500
multiple torsion	0.280/0.500	0.298/0.500

[a] $R = \sum(F_o - F_c)/\sum F_o$. [b] Distances deviating by more than 0.04 Å from their ideal van der Waals contact distances.

or, more likely, a reflection of the presence of bound water molecules or salt. No trace of bound coumarin is observed in the binding pocket. Refinement of this structure as described previously gave an R-factor of 15.6% at 2.7-Å resolution with good geometry (Table I). Seventy-three water molecules were included in the refinement. The active-site residues show very little change in position or orientation after photolysis as compared to the acyl enzyme structure of chymotrypsin–cinnamate B. The γ-oxygen of serine 195 has rotated 0.95 Å back into the binding pocket via a torsion angle rotation of about 40° along the α-carbon–β-carbon bond. The other two members of the catalytic triad (His 57 and Asp 102) appear unchanged, implying that very little side-chain movement between these residues is necessary in order to accomplish acylation and deacylation of substrate or inhibitors. The largest movement in the active site upon deacylation is seen for methionine 192, which appears to rotate toward the interior of the binding pocket upon loss of the cinnamate (the

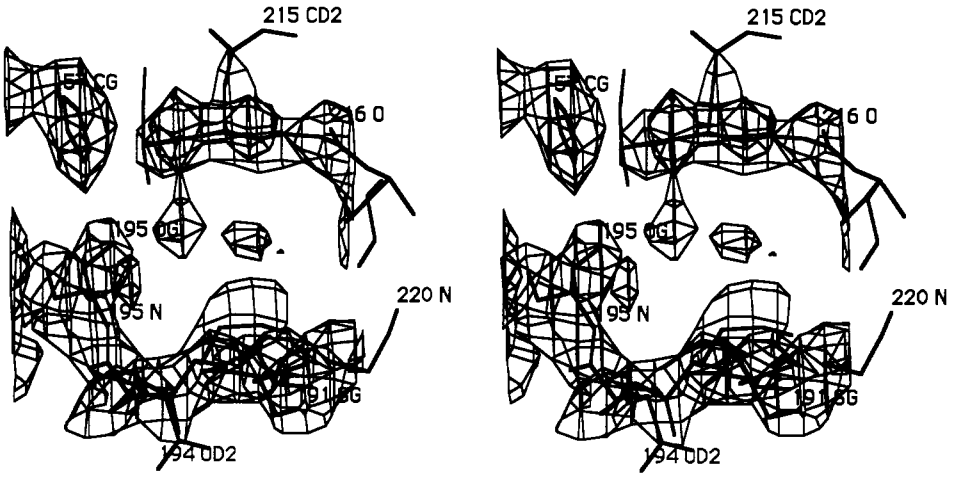

FIGURE 10: Structure of active site of chymotrypsin after photolysis of cinnamate B, viewed in the same orientation as in Figure 8. Note the lack of density in the binding pocket where the planar inhibitor was previously found and the clear truncation of protein density at the γ-oxygen of serine 195. The catalytic triad residues are shown in their refined positions. See Figure 11 and Results for a comparison of active-site residues before and after photolysis.

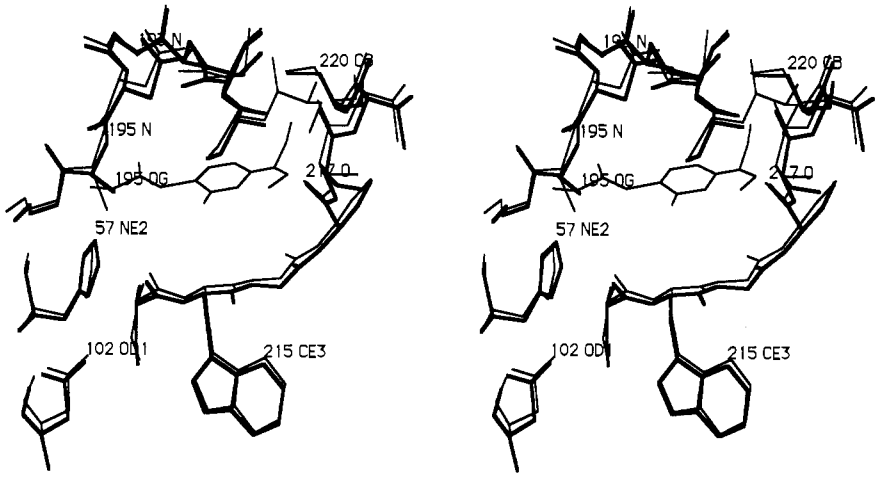

FIGURE 11: Stereo figure showing superimposed active-site residues of chymotrypsin before and after photolysis.

δ-sulfur atom moves by 0.97 Å and the ε-carbon by 1.2 Å). It is possible that this residue plays a role in selecting against positively charged groups and that the iminium ion of the cinnamate forces the side chain to deviate from its preferred conformation. See Figure 11 for a superimposed stereoview of the active-site residues before and after photolysis. The rms difference for all atoms before and after photolysis was 0.41 Å.

.On the basis of the above observations, we can conclude that the observed changes in diffraction intensity for cinnamate B are caused by successful isomerization and deacylation of the inhibitor. In neither case do the protein crystals appear to suffer from their exposure to the beam of the arc lamp. Radiation decay during data collection after photolysis is normal, the crystal unit cell parameters are unchanged, and the protein maps appear unaffected. The beam does not seem to produce excessive heat after passage through the UV filter (even at the point of maximum focusing). Thus, photons appear to be a viable energy source for the triggering of chemical events within a protein crystal.

Discussion

Solution Studies

We have previously studied the photochemistry of the model methyl ether cinnamate, MEC, and ethyl cinnamate, EC, preliminary to our studies of the enzyme system, and we have reported aspects of this photochemistry elsewhere (Porter & Bruhnke, 1989a,b). Photolysis of the methyl ether MEC with 366-nm light results in a rapid decrease in absorbance as the cis photoisomer is formed. The ε of the cis compound is <40% that of the trans at 360 nm. At the photostationary state, the cis photoisomer is 60% of the mixture. Photolysis of EC for 5 min in 98% ethanol/2% Tris buffer, pH 7.4, gives a sharp decrease in the absorbance at 360 nm, followed by a slow increase in absorbance at 380 nm due to the dark formation of the coumarin (DMC). The increase in the absorbance due to the coumarin is first order with $k_c = 7.17 \times 10^{-4}$ s^{-1}. The presence of the cis isomer has been confirmed by NMR after photolysis at <0 °C. The rate of cyclization of *cis*-EC is solvent dependent and increases by 2 orders of magnitude in 50/50 ethanol/Tris buffer. Flash photolysis experiments on *trans*-EC in Tris buffer similar to those described for the acyl enzyme B indicate that *cis*-EC is converted to coumarin DMC with a rate of 1.7 ± 0.5 s^{-1} in this solvent. The yield of coumarin from EC is essentially quantitative under all of the conditions described.

These data support the mechanism for photochemistry of the acyl cinnamate B presented in Figure 1. Absorption of a photon by trans acyl enzyme B results in photoisomerization to cis acyl enzyme B followed by lactonization to the coumarin product and active enzyme with a rate of 3.5×10^3 s^{-1}. The deacylation of the acyl enzyme B cis photoisomer is $>10^9$ faster than the deacylation of the corresponding trans geometric isomer. This result is anticipated by the mechanism presented, since the internal nucleophile on the cinnamate aromatic ring cannot attack the carbonyl of the enzyme serine ester if the alkene is trans. Photoisomerization presents the nucleophile to the reactive site for deacylation and the lactonization of the cis alkene is a rapid process in the enzyme active site.

The two solution experiments presented here (Figures 4 and 5) illustrate two different features of the photochemical system under study. Continuous photolysis of a stirred solution of acyl enzyme with the focused beam of a 500-W mercury–xenon arc lamp (Figure 4) shows that (1) the product ratio of coumarin (photolysis product) to cinnamic acid (hydrolysis product) approaches infinity and (2) the yield of coumarin relative to total acyl enzyme is approximately 1 equiv. These data provide confirmation of the mechanism shown in Figure 1 but do not speak to true kinetics of the isomerization or of the enzymatic recovery of activity after photolysis. The fact that the ratio of recovered activity to the activity of an equivalent amount of uninhibited enzyme does not reach 1.0 (but instead reaches an upper limit of approximately 0.96) shows that a small percentage of activity is lost due to two possible effects: nonreversible photolytic damage of the enzyme and inhibition of enzymatic activity by the liberated (diethylamino)methylcoumarin, which is known to be a weak inhibitor of serine protease activity. These possibilities are currently being explored further.

The fast UV kinetic experiment (Figure 5) shows us that under ideal conditions (aqueous solution, physiological pH, submillisecond irradiation of the entire molecular population) the deacylation of the enzyme occurs in approximately 2 ms, with the formation of a free enzyme–product complex. Since the experiment measures the formation of coumarin directly, these kinetic constants are relevant to processes occuring in the active site but do not necessarily provide kinetic data for the recovery of activity due to product release. Since release of the bound coumarin could be significantly slower than the lactonization process, the true rate of triggering in the active site might be slower than indicated in Figure 5.

Crystallographic Studies and Applications

Aspects of Structural Studies on Chymotrypsin. One extremely important concern regarding any structural studies of chymotrypsin bound with competitive inhibitors is the presence of a tightly associated tetrapeptide observed in the active site of "native" chymotrypsin (Dixon & Matthews, 1989; Almo et al., 1989). This naturally occurring inhibitor was originally observed in the initial structure of γ-chymotrypsin (used in the refinement of the structures reported here) but was mistakenly modeled as a string of water molecules. This endogenous peptide presents concern for two reasons:

(1) It has been shown to block binding of inhibitors such as proflavin and isatoic anhydride (Almo et al., 1989), raising the possibility that any structure of inhibited chymotrypsin solved by X-ray crystallography might contain a significant percentage of active sites occupied by peptide rather than the compound of interest. The tight binding of the peptide creates a great deal of difficulty when trying to soak various active-site compounds into crystals of chymotrypsin, a problem that has been overcome in the past through very extensive soaking of inhibitor. The initial electron density maps of chymotrypsin soaked with cinnamate A and B were immediately and extensively compared with maps of the chymotrypsin–peptide complex (provided by Steven Almo) in order to ensure that the active-site electron density was in fact a clean view of cinnamate acyl enzyme. These comparisons were carried out with the initial unrefined difference maps described above as well as on difference Fourier syntheses calculated after refinement of the structure.

The density for the inhibitors prepared according to the final soaking conditions described previously is clearly truncated around the molecular boundaries of the inhibitors, with no extraneous density that might correlate with the density observed for the tetrapeptide. Soaking with the less reactive cinnamate B, however, does appear to lead to significant retention of peptide when the soak is performed for shorter periods of time or with concentrations of inhibitor less than 100 mM, as shown by our first unsuccessful attempts to solve the structure of chymotrypsin inhibited with this compound

(unpublished data). The results of these studies leads us to conclude that crystals of γ-chymotrypsin prepared as described previously are fully occupied by the cinnamate acyl enzyme complex and that the peptide has been successfully displaced.

(2) The model used as the starting structure in all our refinements was the set of coordinates of γ-chymotrypsin provided by Cohen et al. (1981) to the Brookhaven Protein Data Bank for crystallographic coordinates. As pointed out by a reviewer, these coordinates, while correct regarding the general architecture of the molecule, are flawed regarding the true structure of the active site, which is clearly different than the PDB model. This concern raises the following points regarding the use of the Davies model in our work:

(i) As stated in the first paper of this series (Stoddard et al., 1990), the active site was "built and analyzed...using initial coordinates taken from the Brookhaven PDB". This initial round of rebuilding was performed in order to correct any inconsistencies with our structure that might be observed due to the presence of peptide in the structure used to provide phases for our unrefined maps. No water molecules were included in the map calculation or in the subsequent refinements in order to avoid ambiguities regarding the structure of the active site.

(ii) The PDB structure of chymotrypsin, while in error regarding the presence of an endogenous peptide in the active site, is fairly accurate regarding the positions of the active-site residues in the enzyme. As shown in our results, as well as in previous structures of inhibited chymotrypsin (Segal et al., 1971), the binding-site residues of this enzyme appear to be relatively unaffected structurally by the binding and release of substrate or inhibitor, implying that catalysis (or binding of peptide) occurs with relatively small movements in the active site. While the presence or absence of specific interactions such as the Ser 195–His 57 hydrogen bond in the native structure may be unresolved, the overall conformation of the active site is quite clear, allowing structural studies of the type reported here.

A second concern regarding our structural studies is the relatively fast "dark" deacylation of cinnamate A observed in solution ($k_{deac} = 10^{-3}$ s^{-1}), which actually made preparation of 100% activity-free chymotrypsin impossible in solution. Over the course of the crystal soak, the inhibitor might reasonably be expected to deacylate nonphotochemically, producing a structure that actually shows the product of the hydrolysis reaction. The evidence against this occurring in the crystal is 3-fold:

(i) Difference maps calculated before and after refinement clearly show a strong covalent bond between the serine γ-oxygen and the cinnamate carbonyl. This observation is independent of the presence of inhibitor coordinates in the model used for refinement and also of any restraints used in the refinement.

(ii) The inhibitor density is not affected by flowing approximately 10 mL of inhibitor-free mother liquor over the crystal during photolysis and data collection (roughly a 100000-fold excess by volume). This is as opposed to the loss of inhibitor observed for the identical experiment performed with cinnamate B, implying that the relative rates of reactivity in the dark and light for the two compounds are consistent with the retention of covalently bound inhibitor in the absence of irradiation.

(iii) Binding of alternate mechanism-based inhibitors, such as 3-benzyl-6-chloro-2-pyrone, to chymotrypsin bound with cinnamate is dependent on the photolysis of the crystal, implying that deacylation/reacylation in the crystal is caused by the photoisomerization of covalently bound cinnamate (Stoddard et al., unpublished results).

These results confirm a widely held observation that the reactivity of covalent enzyme–substrate or enzyme–inhibitor complexes is often drastically altered in the crystalline form. In the specific case of chymotrypsin, Almo et al. (1989) have stated that formation of a stable acyl enzyme may be explained by a nonproductive orientation of the complex (observed for the cinnamate structures), as well as by the relative inaccessibility of the active site to bulk solvent.

Applications of Photochemical Methods in Structural Studies. It is apparent from the results of our studies of photoreversible cinnamate inhibitors in solution that such compounds, if designed properly, should make effective triggers for the regeneration of free serine protease active site from inhibited enzyme, a technique that should be useful for many other families of enzymes. We are interested in applying these methods to protein crystallography and in using such compounds for the simultaneous initiation of catalysis by the enzyme in the crystalline state. Isomerization of inhibitor and formation of coumarin product in the inhibited complex in solution occur on a submillisecond time scale, theoretically fast enough to trigger the accumulation of rate-limited intermediates in the crystal. In experimental terms, however, whether synchronized activation of the enzyme means that one can observe a similarly concerted accumulation of intermediate chemical states during catalysis depends on the thermodynamics of the system and the time course of the process to be followed. The Maxwell–Boltzmann energy distribution for a population of a given molecular species states that the percentage of molecules which possess enough total energy to cross a kinetic barrier decreases exponentially in relation to the absolute magnitude of the barrier, in this case the E_{act} for acylation by chymotrypsin. Assuming an approximate overall energy of activation for serine proteases of 10–15 kcal/mol and a time course for the corresponding chemical event in the picosecond range, it is obvious that formation of the initial chemical intermediate will not proceed with quantitative yield over the lifetime of the intermediate and that this yield will decrease as the lifetime of the intermediate decreases. Equally obvious is that for each kinetic barrier present in the reaction pathway, the yield of a given intermediate (defined as the percentage of molecules found in that particular intermediate state relative to all molecules in the crystal) will decrease as a multiplicative function of the chemical efficiency of each individual kinetic step. Therefore, the probability of forming and observing a transient intermediate state in the crystal is strictly dependent on the efficiency of the triggering step, the magnitude of each kinetic barrier leading into the intermediate, the corresponding energy state of the catalytic system, the lifetime of the intermediate of interest, and the investigators' ability to collect the necessary data within a single turnover of the enzyme in the crystal. Thus, observation of the ATP-bound Michaelis complex of *ras* p21 (half-life of approximately 20 min) is possible upon initiation of catalysis by flash photolysis (Almo et al., in preparation), whereas the observation of acylated intermediates of chymotrypsin–ester substrate complexes (half-lives of approximately 0.01–1 s in solution) is a much more difficult proposition.

It is apparent from the results obtained for the irradiation of chymotrypsin inhibited by cinnamates A and B that the primary considerations for the use of light-induced triggers are the rate of the photoreaction, the efficiency of the trigger when bound to the enzyme and the possibility of competitive UV absorption by the protein, the rate of product release and

activity regeneration, photodegradation of enzyme upon photolysis, and damage of the crystalline specimen when the experiment is carried out in the crystal. It is clear that photochemistry does occur in the enzyme active site, both in solution and in the crystal, and that binding of the inhibitors by enzyme does not by itself appear to affect the isomerization, as can be seen by the rate of coumarin formation for cinnamate B in the presence and absence of chymotrypsin. This implies that the enzyme, at least in solution, shows a high enough dynamic range of motion or "breathing" to allow isomerization in the active site.

Although the protein does not physically impede the photochemical reaction of the cinnamate in the active site, the binding of inhibitor by protein may shield the compound from isomerization through competitive absorption of UV light of the necessary wavelength. Figure 2 shows the relative molar absorptivity of cinnamates A and B and of the acyl enzyme of the amino-substituted inhibitor. Chymotrypsin shows a molar absorptivity at 280 nm almost twice that of the absorption band of cinnamate B at 360 nm. For the unsubstituted cinnamate A, which has the same peak but with a much smaller intensity and shifted to approximately 300 nm, the photoefficiency of triggering is greatly reduced by an internal filter effect caused by protein absorbance at the same wavelength. We can see, therefore, that there are two compelling reasons for designing the system to operate in the region around 350 nm: reduction of protein absorbance when the inhibitor is bound to the enzyme and reduction of ultraviolet damage to the system under study.

The process of photodriven isomerization is an interesting one to carry out in the protein crystal. The effective concentration of protein in the crystal is much higher (approximately 5–100 mM), compounding our concerns regarding protein absorption. Moffat (1989) has shown that for a photochemical trigger in the protein crystal to operate efficiently (100% regeneration of active enzyme in less than 1 ms), the transmittance of light through the crystal generally needs to be greater than 90%, corresponding to an optical density of 0.06. This means the extinction coefficient of the crystal must be less than 0.1 mM^{-1} cm^{-1}, corresponding to a crystal thickness of 200 μm and an effective protein concentration of 30 mM. We can see that the absorption of chymotrypsin is close to zero at 350–380 nm, meeting the above criteria. We can aid the system by irradiating through the narrowest dimension of the crystal.

The studies presented in this paper do not present any evidence that the regenerated chymotrypsin is still active in the crystal after photolysis of the inhibitor. Work currently in progress, however, shows that the photolysis of the complex yields enzyme which is capable of binding mechanism-based inhibitors such as 3-benzyl-6-chloro-2-pyrone both in solution and in the crystal on a time scale consistent with previously published results for those compounds, evidence that regenerated enzyme is capable of recognizing and binding phenyl substrate analogues and undergoing acyl attack in a manner similar to native enzyme (Stoddard et al., in preparation).

Our studies show that, under the appropriate photochemical conditions as described above, photoisomerization in the protein crystal is possible and proceeds on a reasonable time scale. This has important implications for enzymatic function in the crystal, which is obviously a much less restricted environment than is often thought. Protein crystals can contain from 20% up to 80% water by volume (Hajdu et al., 1988), providing a specimen of protein slightly more dense than that of the intracellular environment (70–80% water w/w). Thus photoreactive compounds should provide an avenue into kinetic studies in the protein crystalline state, using any of a number of techniques including solid-state NMR, absorption spectroscopy, and polychromatic X-ray crystallography. What is truly desirable for fast kinetic studies in such systems is a submillisecond chemical trigger; for this reason photochemical activation is perhaps the most promising technique. The goal is to present the enzyme with all conditions necessary for competent turnover but to "cage" one chemical component of turnover behind the bars of an organic trap—bars that can be removed with photons. The strategies under current investigation can be divided into two broad categories, all of which have been reported to some degree in the literature [a concise review was written by Ogden (1988)].

(*i*) *Caged Cofactor or Substrate.* A number of photoreversible cages of catalytically important ions such as calcium and magnesium have been developed in the past 2–3 years, which have K_D's for various ionic species in the nanomolar range and which therefore compete very effectively with many enzymatic systems for metal binding. The photoreversible chelator DM-nitrophen, based on methoxynitrophenyl derivatives of EDTA (Morad et al., 1988), has been developed to study cation transport across the membrane. A different class of light-reactive cages, based on the chelator BAPTA, has been developed by Tsien, Adams, and co-workers (Adams et al., 1988) to study calcium-dependent conductance in neurons and other systems. These compounds are just beginning to be investigated as possible triggers in protein crystals.

Possibly the best investigated group of photoreleasable biomolecules is a large family of nitrobenzyl derivatives such as (2-nitrophenyl)ethyl esters of ATP, ADP, GTP, cAMP, and inositol 1,4,5-triphosphate (Walker et al., 1987, 1988; Nerbonne, 1986; McKay et al., 1980). Upon irradiation, these compounds release a weakly acidic effector molecule (such as a nucleic acid phosphate ester) with a very high quantum efficiency. These molecules also were originally developed for studies of cellular phenomena such as muscle contraction (Goldman, 1987), second messenger regulation (Niedergerke & Page, 1977), and neurotransmitter action (Dolphin, 1988). This group is also probably the best studied in relation to its possible use in X-ray crystallography.

In the context of their possible use as chemical triggers for single-crystal diffraction studies, both of the above families of compounds suffer from one drawback: the act of photoactivation causes a release of extraneous organic byproducts into the crystal at relatively high concentrations (diacetic acid derivatives in the case of DM-nitrophen, or nitrosophenyl ketones when 2-nitrobenzyl cages are used). These compounds have been shown to be reactive against protein and damaging to the crystal unless care is taken to provide a special chemical environment that minimizes unwanted reactions (such as the use of a highly reducing mother liquor for crystals of *ras* oncogene product p21 during the photolysis of caged GTP—G. Petsko et al., in preparation). These considerations bring us to the method under study in this paper.

(*ii*) *Caged Enzyme.* All enzymatic inhibitors are examples of chemical cages that capture, block, or restrain catalytically essential residues. Recently, however, an assortment of compounds have arisen with the additional property of photoreversibility, such as the phenyl cinnamates of this study. These compounds are light-dissociable cages that act by trapping the nucleophilic serine found in all serine proteases. Their deacylation rates can be tremendously increased through irradiation by light of the appropriate wavelength and intensity, which results in isomerization about the carbon–carbon double

bond, acyl attack by the phenyl hydroxyl, cyclization, liberation of active enzyme, and loss of unreactive product. For the purpose of initiating turnover in the crystal, these cages offer the advantage of not producing damaging byproducts that would have to be protected against. Crystallographically, the compounds of our study offer the additional advantage of being covalently bound to the enzyme itself and therefore being just as observable crystallographically as substrate. This offers enormous potential for observing the triggering process of interest.

In conclusion, the photochemical destruction of a covalently bound inhibitor has been shown in theory and in practice as a possible method for the triggering of enzymatic intermediate accumulation both in solution and in the crystal. When the system is properly designed and studied, such methods should be applicable to the study of short-lived intermediate states by X-ray crystallography and other biophysical techniques.

ACKNOWLEDGMENTS

We thank Dr. S. Atherton for help with the flash photolysis studies. Special thanks are given to the laboratories of Drs. Alex Rich, Bob Field, and Mark Wrighton for the use of equipment and for advice rendered.

Registry No. Chymotrypsin, 9004-07-3.

REFERENCES

Adams, S. R., et al. (1988) *J. Am. Chem. Soc. 110*, 3212–3220.

Almo, S. C., Howell, P. L., Petsko, G. A., & Hajdu, J. (1989) *Proc. Natl. Acad. Sci. U.S.A.* (submitted for publication).

Battels, E., Wasserman, N. H., & Erlanger, B. F. (1971) *Proc. Natl. Acad. Sci. U.S.A. 68* (*8*), 1820–1823.

Berezin, I. V., Varfolomeyev, S. D., & Martinek, K. (1970) *FEBS Lett. 8* (*4*), 173–175.

Berezin, I. V., Varfolomeyev, S. D., Klibanov, A. M., & Martinek, K. (1974) *FEBS Lett. 39* (*3*), 329–331.

Bieth, J., Wassermann, N., Vratsanos, S. M., & Erlanger, B. F. (1970) *Proc. Natl. Acad. Sci. U.S.A. 66* (*3*), 850–854.

Cohen, G. H., Silverton, E. W., & Davies, D. R. (1981) *J. Mol. Biol. 148*, 449–479.

Dixon, M. M., & Matthews, B. W. (1989) *Biochemistry 28*, 7033–7038.

Dolphin, A. C., et al. (1988) *Pfluegers Arch. 411*, 628–636.

Goldman, Y. A. (1987) *Annu. Rev. Physiol. 49*, 637–654.

Gurney, A. M., Tsien, R. Y., & Lester, H. A. (1987) *Proc. Natl. Acad. Sci. U.S.A. 84*, 3496–3500.

Hajdu, J., Acharya, K. R., Stuart, D. I., Barford, D., & Johnson, L. N. (1988) *Trends Biochem. Sci. 13* (*3*), 104–109.

Kaufmann, H., Vratsanos, S. M., & Erlanger, B. F. (1968) *Science 162*, 1487–1488.

Konnert, J. H., & Hendrickson, W. A. (1980) *Acta Crystallogr. A36*, 344–350.

McKay, J. A., Herbette, L., Kihara, T., & Trentha, P. R. (1980) *Proc. Natl. Acad. Sci. U.S.A. 77* (*12*), 7237–7241.

Moffat, K. (1989) *Annu. Rev. Biophys. Biophys. Chem. 18*, 309–332.

Morad, M., et al. (1988) *Science 241*, 842–844.

Neidergerke, R., & Page, S. G. (1977) *Proc. R. Soc. London, B 197*, 333–362.

Nerbonne, J. M. (1986) in *Optical Methods in Cell Physiology* (de Weer, P., & Salzberg, B., Eds.) pp 417–455, Wiley, New York.

Ogden, D. (1988) *Nature 336*, 16–17.

Porter, N. A., & Bruhnke, J. (1989a) *J. Am. Chem. Soc. 111*, 7616–7618.

Porter, N. A., & Bruhnke, J. (1989b) *Photochem. Photobiol.* (in press).

Segal, D. M., Powers, J. C., Cohen, G. C., Davies, D. R., & Wilcox, D. E. (1971) *Biochemistry 10*, 3728–3741.

Stoddard, B. L., Bruhnke, J., Porter, N. A., Ringe, D., & Petsko, G. (1990) *Biochemistry 29*, 4871–4879.

Turner, A. D., Pizzo, S. V., Rozakis, G., & Porter, N. A. (1987) *J. Am. Chem. Soc. 109*, 1274–1275.

Turner, A. D., Pizzo, S. V., Rozakis, G., & Porter, N. A. (1988) *J. Am. Chem. Soc. 110*, 244.

Varfolomeyev, S. D., Klibanov, A. M., Martinek, K., & Berezin, I. V. (1971) *FEBS Lett. 15* (*2*), 118–120.

Walker, J. W., et al. (1987) *Nature 327*, 249–252.

Walker, J. W., Reid, G. P., Ray, J. A., & Trentham, D. R. (1988) *J. Am. Chem. Soc. 110*, 7170–7177.